Long-range coherence of interacting Bose gas of dipolar excitons

2007 J. Phys.: Condens. Matter 19 295209

(http://iopscience.iop.org/0953-8984/19/29/295209)

IOP PUBLISHING JOURNAL OF PHYSICS: CONDENSED MATTER

J. Phys.: Condens. Matter **19** (2007) 295209 (22pp) doi:10.1088/0953-8984/19/29/295209

Long-range coherence of interacting Bose gas of dipolar excitons

V B Timofeev, A V Gorbunov and A V Larionov

Institute of Solid State Physics, Russian Academy of Sciences, 142432 Chernogolovka, Russian Federation

E-mail: timofeev@issp.ac.ru

Received 17 April 2007
Published 11 June 2007
Online at stacks.iop.org/JPhysCM/19/295209

Abstract

Experiments connected with dipolar exciton Bose condensation in lateral traps are reviewed. Observations of long-range coherence of condensate in ring electrostatic traps in Schottky-diode heterostructures with double and single quantum wells are presented and discussed.

(Some figures in this article are in colour only in the electronic version)

1. Introduction

Hydrogen-like excitons in intrinsic semiconductors are known to be electrically neutral and the energetically lowest electronic excitations. For a dozen decades excitons have been used as a convenient and very efficient tool to simulate the behaviour of matter under the effect of density variation and external impacts, such as temperature, magnetic and electric fields, deformation potential, etc.

Depending on the concentration of electron–hole (e–h) excitations and temperature, experiments with bulk intrinsic semiconductors were used to realize the situation of a weakly interacting exciton gas, a molecular exciton gas (gas of biexcitons and excitonic trions), a metallic electron–hole liquid, and a dense neutral electron–hole plasma.

The exciton is a sort of composite boson because it consists of two fermions, an electron and a hole, and this accounts for the resultant exciton spin being integer valued. This led to the hypothesis formulated in the early 1960s [1–3] that Bose–Einstein condensation (BEC) is possible to observe, in principle, in a weakly nonideal and sufficiently diluted excitonic gas in semiconductors at rather low temperatures. In the limit of diluted excitonic gas, $na_{\mathrm{ex}}^{d} \ll 1$, where n is exciton density, a_{ex} is the exciton Bohr radius, and d is the dimensionality of the system under consideration. The Bose–Einstein condensation of indistinguishable excitons suggests macroscopic occupation of the exciton ground state with zero momentum and the appearance of a spontaneous order parameter (coherence) in the condensate [4–6].

In the limit of high e–h density, $na_{\mathrm{ex}}^{d} \gg 1$, the exciton concept used to be regarded by Keldysh and collaborators [4–6] in direct analogy to Cooper pairs, and the condensed excitonic

state (a sort of excitonic insulator state) was described in the mean-field approximation by analogy with the Bardeen–Cooper–Schrieffer superconducting state. The sole difference consisted in the fact that the pairing in an excitonic insulator was determined by the e–h interaction and the excitons themselves served as an analogue of the Cooper pairs [4]. Well apparent Coulomb gaps in the excitonic insulator state can arise under nesting of the electron–hole Fermi surfaces. Theoretical studies reported in [7] suggest a smooth transition between the low- and high-density limits.

BEC was discovered decade ago in the diluted and deeply cooled gases of atoms whose resulting spin is integer valued [8]. This striking discovery was possible owing to the elegant realization of the laser and evaporative cooling techniques in their application to diluted atomic gases and to the selective small-volume accumulation of atoms in magnetic traps. The transition temperatures T_C in the case of alkaline atomic gases turned out to be very low (around 1 μK and even lower), which is due to the large masses of atoms and their relatively low densities resulting from the inevitable losses during cooling and accumulations in traps. After BEC had been found in the diluted gases of bosonic atoms, this phenomenon stimulated special interest and acquired significance with reference to excitons. Indeed, the translational effective masses of excitons in semiconductors are typically small, smaller than the mass of a free electron. Therefore, unlike BEC in diluted gases of atomic hydrogen, alkalis, and transition metals, BEC in an excitonic gas at experimentally achievable densities may occur at much higher temperatures (e.g. liquid helium temperature range). However, excitonic gas being a photo-excitable and, in principle, nonequilibrium system, the problem of its cooling to temperatures of the crystal lattice serving as a thermostat assumes importance.

In bulk semiconductors BEC has not been observed until now in spite of extensive attacks on this problem and impressive experiments performed, in particular, on long-living para- and orthoexcitons in Cu_2O (see, for instance, [9–11]) and spin-aligned excitons in uniaxially compressed Ge (analogue of spin-aligned hydrogen atoms). The search for excitonic BEC in bulk semiconductors is at present still in progress.

In recent years, the BEC of excitons has been extensively investigated in two-dimensional (2D) systems based on semiconductor heterostructures. The studies are focused on two-dimensional objects with spatially separated electron–hole layers. Researchers were attracted to these objects by theoretical works done in the mid-1970s [12, 13]. In the context of the problem under consideration, double quantum wells (DQWs) turned out to be the most interesting among other two-dimensional objects based on semiconductor heterostructures because they allow the photoexcited electrons and holes to be spatially separated between adjacent QWs (for instance see [14–22]). In DQWs under applied bias in the growth direction, tilting quantized subbands, it is possible to excite excitons whose electrons and holes are in different QWs separated by a transparent tunnel barrier. Such an exciton is called a spatially indirect or interwell exciton (I), as opposed to a direct (D) or intrawell exciton in which electron and hole are placed within the same QW (figure 1). A situation realized in GaAs/AlAs heterostructures where excitons are not only spatially separated but also prove to be indirect in momentum space was considered in [17]. Interwell excitons have a longer lifetime than intrawell ones because of limited overlap between electron and hole wavefunctions through the tunnel barrier. Characteristic times of the radiative recombination of IEs are as large as dozens and even thousands of nanoseconds. Therefore, they are easy to accumulate, and the gas of interwell excitons can be cooled to rather low temperatures close to the temperature of the crystal lattice. It is worthwhile to make a note that thermalization of two-dimensional excitons, and interwell excitons in particular, involves bulk phonons. In this case, however, the law of momentum conservation along the quantization axis is relaxed, which accounts for the lack of a 'bottleneck' for the recoil on small momenta and the feasibility of one-phonon relaxation with participation

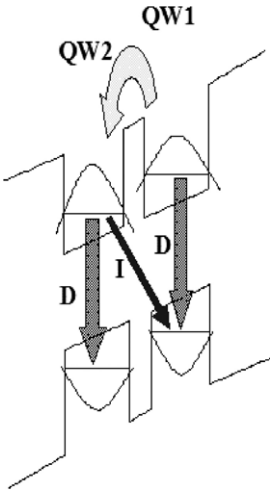

Figure 1. Schematic representation of the energy levels in coupled double quantum wells under applied electric field. Arrows indicate intrawell (D) and interwell (I) optical transitions.

of acoustic phonons even at $T \leqslant 1$ K. As a result, the relaxation of IEs to the lattice temperature takes place a few orders of magnitude faster than their radiative decay [23, 24]. Because of the broken inverse symmetry, interwell excitons have a large dipole moment even in the ground state (due to this these excitons are often called dipolar). As the result of this, such excitons cannot be bound into molecules or other complicated complexes due to dipole–dipole repulsion, and, consequently, cannot condense, in principle, into a liquid state.

BEC in a 2D exciton gas can occur only under lateral confinement. By collecting excitons in a lateral trap, a lower total flux of excitons, i.e. lower pumping power, is required. The critical temperature for the case of interwell excitons confined in a lateral trap with rectangular barriers is given by the expression

$$T_{\mathrm{C}} = \frac{2\pi\hbar^2 N_{\mathrm{ex}}}{g_{\mathrm{ex}} k_{\mathrm{B}} m_{\mathrm{ex}} \ln(N_{\mathrm{ex}} S/g_{\mathrm{ex}})}, \tag{1}$$

i.e. it decreases logarithmically with increasing area S occupied by two-dimensional Bose particles with density N_{ex}, translational effective mass in the plane m_{ex}, and degeneracy factor g_{ex} (k_{B} is the Boltzmann constant). By way of example, the critical temperature T_{C} of the interwell exciton gas in GaAs/AlGaAs DQWs with the density 10^{10} cm^{-2} and translational mass 0.25 m_0 (m_0 is the bare electron mass) under a micron-scale lateral trap is around 2 K.

The spatial confinement in the QW plane may be related to large-scale random potential fluctuations due to variations of the QW width on heteroboundaries— $w(R)$. Also related to these variations are changes in the effective lateral potential $U(r) = U(w(r))$ [25]. Under quasi-equilibrium conditions, the exciton density distribution is described by the equality $\mu(N(r)) + U(r) = \overline{\mu}$, where the chemical potential of interwell excitons $\overline{\mu}$ is related to their average density and $\mu(N)$ is the chemical potential of a homogeneous excitonic phase in the spatially confined region (in a trap). Evidently, $|\mu(r)| < |\overline{\mu}|$ because $\mu(N) = -|E_{\mathrm{ex}}| + |\delta U|$ (E_{ex} is the exciton binding energy). This means that excitons more easily accumulate in the lateral confinement region, where their density can be much in excess of the mean density in

the QW plane. Therefore, critical conditions corresponding to the Bose condensation on IEs are most readily realized in lateral domains that function as exciton traps.

A variety of scenarios of collective behaviour in a sufficiently dense system of spatially separated electrons and holes were theoretically considered in [26–33]. For example, it was claimed in [29] (see also [32]) that a liquid dielectric excitonic phase may constitute the metastable state in an e–h system despite the dipole–dipole repulsion of interwell excitons at certain critical parameters, such as the dipole moment, density and temperature. As shown in [25], the condensed dielectric excitonic phase can arise only in the presence of lateral confinement in the DQW plane. Such confinement and the associated external compression facilitate the accumulation of interwell excitons to critical densities sufficient for the effects of collective exciton interaction to be manifested. In [28] the role of spin degrees of freedom under Bose condensation is discussed.

In the theoretical work published recently it was shown [31] that Bose condensation in a trap results in a dramatic change of the interwell exciton photoluminescence angular distribution. Due to long-range coherence of condensed phase a sharply focused peak of luminescence in the direction normal to the DQW plane should appear. The radiation peak should exhibit strong temperature dependence due to the thermal order parameter fluctuations across the system. The angular distribution of photoluminescence can also be used for imaging vortices in trapped condensate, because vortex phase spatial variations lead to destructive interference of photoluminescence intensity in certain directions, creating nodes in intensity distribution that imprint the vortex configuration.

Real heterostructure systems with quantum wells always contain a fluctuating random potential due to the presence of residual impurities, both charged and neutral, as well as a variety of structure defects. These imperfections create a random potential relief in the QW plane; as a result, photoexcited electrons and holes specially separated between adjacent QWs (as well as interwell excitons) may be strongly localized on these fluctuations at sufficiently low temperatures. Such an effect of strong localization in coupled quantum systems is manifested, for example, as thermally activated tunnelling of localized particles [18]. In connection with this, investigations of the properties of delocalized excitons (above the 'mobility edge') are carried out in perfect structures with a minimum density of localized states (in high-quality structures around or even less than 10^9 cm^{-2}).

2. Experimental details

Now we consider a few experiments conducted recently using n–i–n GaAs/AlGaAs heterostructures with DQWs that have large-scale random potential fluctuations and GaAs/AlGaAs Schottky-diode structures with DQWs and single QWs, where interwell (dipolar) excitons (IEs) exhibit collective behaviour after the critical density and temperature are achieved [20, 22, 34–37, 42, 43].

Firstly, we describe the architecture of the used n–i–n heterostructure with DQWs. Double quantum wells 12 nm in thickness were separated by a narrow barrier of four AlAs monolayers. Similar AlAs epitaxial layers were grown on the borders between each QW and AlGaAs insulating barriers of 150 nm thickness. Built-in electrodes were n^+-GaAs (Si doped) layers of 100 nm thickness. Large-scale random potential fluctuations were induced in these structures using the growth interruption technique at the boundaries of the AlAs and AlGaAs barriers.

The main information about interwell exciton properties has been obtained by analysis of luminescence spectra, such as excitation power, temperature, electric field, and polarization of resonant optical pumping varied under steady-state or pulse optical excitation.

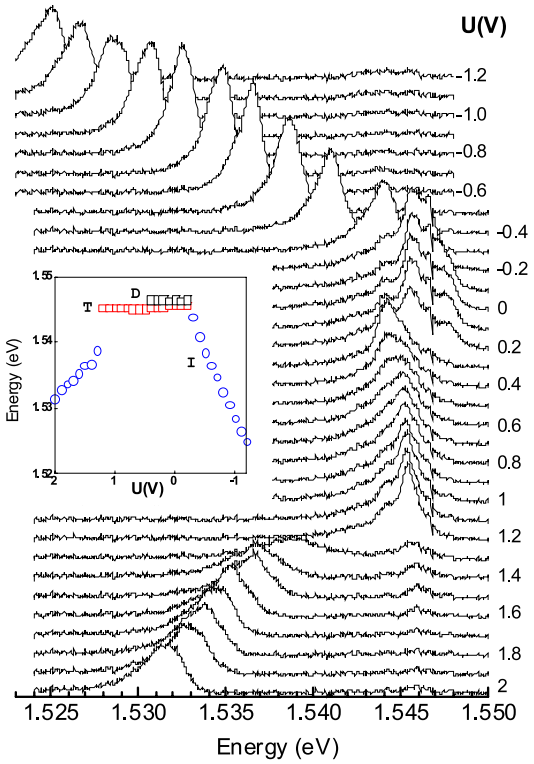

Figure 2. Luminescence spectra of intrawell excitons (D), trions (T), and interwell excitons (I) in DQWs at different bias voltages U (U values in volts are given near the corresponding curves). The inset shows the dependence of spectral positions of maxima of corresponding lines on electric field. $T = 2$ K.

2.1. Phase diagram

Let us start with an illustration of the quality of used structures with DQWs. The optical transitions of interest are schematically presented in figure 1. Luminescence spectra of IEs measured at different biases are depicted in figure 2. The intrawell luminescence region at zero electric bias exhibits two lines. One is 1s HH of the free heavy-hole exciton (denoted as D) and the other is the line of bound, charged excitonic complexes (intrawell excitonic trion, T). At a small bias, it is possible to change both the charge and the structure of the excitonic trion by varying the sign of the gate voltage. The line of heavy-hole interwell excitons (I line) emerges in the spectra after the electric field is switched on and causes the Stark shift of the dimensionally quantized bands in adjacent QWs to be $eF\Delta z \geqslant E_{\mathrm{D}} - E_{\mathrm{I}}$ (E_{D} and E_{I} are the intrawell and interwell exciton binding energies, respectively, F is the electric field, and Δz is the distance between the electron and hole in the interwell exciton). The shifts of the I line are almost linear upon a change in electric field at both positive and negative voltages between the electrodes—n^+ doped regions (see the inset to figure 2). This line can be displaced along the energy scale over a distance almost a dozen times as large as the interwell exciton binding energy. At high electric voltage and steady-state excitation, the I line in the luminescence spectra predominates. Under the same conditions, the luminescence of intrawell excitons (D) and charged excitonic complexes (T) is several orders of magnitude weaker. A large quantum

yield of IE luminescence in the studied structures suggests their high quality. This ensues from the fact that a rise in the applied bias causes the IE lifetime to increase by a factor of ten or even more while the intensity of luminescence remains practically unaltered (see figure 2).

Now briefly consider changes in the IE luminescence spectra at various pumping values under steady-state excitation by a Ne–He laser focused to a spot of about 10 μm at the sample surface [20]. The I line at sufficiently low temperatures ($T = 0.81$ K) and small excitation powers around 100 nW is broad ($\approx$2.5 meV) and asymmetric, with a large long-wave 'tail' and clear-cut violet boundary. Such properties of the IE photoluminescence line result from the effect of strong exciton localization on random potential fluctuations due to the presence of residual impurities. In this case, the line width reflects the statistical distribution of the chaotic potential amplitudes. As the pumping power increases, a narrow line (FWHM around 1.2 meV) starts to emerge in a threshold manner at the 'blue' edge of the spectrum. The intensity of this line increases superlinearly near the threshold in accordance with a near-quadratic law. It is only at high-power pumping that the superlinear growth of the intensity changes to a linear one, and the line starts to broaden and extend to higher energies. The shift of the line towards the high energies suggests screening of the applied electric field when IE density becomes sufficiently high. Then, the experimental measurements of this shift allow us to estimate the interwell exciton density as above using the Gauss formula for the spectral shift $\delta E = 4\pi e^2 n \Delta z/\varepsilon$ (n is the exciton density and ε is the dielectric permittivity). With this approach, the IE concentration is $n = 3 \times 10^{10}$ cm^{-2} when the line is shifted by less than 1.3 meV. A sufficiently narrow IE luminescence line can be seen at various negative bias voltages in the range from -0.5 to -1.2 meV.

Direct evidence of the interwell exciton condensation was obtained in experiments with single trapping domains associated with large-scale fluctuations of random potential. The experiments were conducted using n–i–n structures of the described architecture covered with a 100 nm thick metallic layer (Au–Cr film), which plays the role of a shadow mask. The film was etched using electron beam 'lift-off' photolithography to fabricate circular windows with a minimum diameter around 1 μm. These windows were used to excite and record luminescence signals. The metallic mask in such experiments did not contact with the n$^+$-doped contact layer of the heterostructure.

The results exhibited below were obtained by optical excitation and subsequent detection of luminescence directly through windows 1 μm in diameter (figures 3(a), (b)). The experiments were carried out under resonant excitation of intrawell excitons with heavy holes (1s HH-intrawell excitons) by a tunable Ti–Sp laser in order to overheat minimally the excitonic system relative to the lattice temperature. At small excitation densities (below 40 μW), the luminescence spectra exhibit a relatively broad (some 2 meV) asymmetric IE band (figure 3(a)). This inhomogeneously broadened line is due to strongly localized excitons. As the pumping increases ($\geqslant$50 μW), a narrow line emerges in a threshold manner at the 'blue' edge of the broad band. The intensity of this line grows superlinearly with increasing pumping (see the inset to figure 3(a)). The minimal measured total width of this line in the experiments was about 250 μeV. It was close to the lattice temperature. A further rise in pumping power (to over 0.5 mW) led to a monotonic broadening of the narrow IE line and its shift towards higher energies (effect of the external electric field screening).

In these experiments, the narrow IE line disappeared from the spectrum at $T \geqslant 3.6$ K. Figure 3(b) illustrates the typical behaviour of the I line upon temperature variations and fixed pumping. One can see that at $T = 1.8$ K and excitation power 250 μW this high-intensity line evidently rises above the structureless background of localized excitons. Its intensity drops with increasing T without a substantial change in the width; at $T = 3.6$ K it is becoming practically indiscernible against the background of the structureless spectrum.

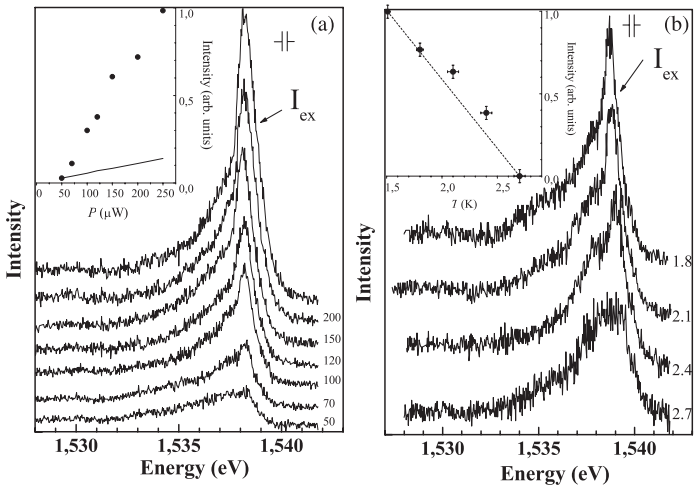

Figure 3. Interwell exciton luminescence spectra in a sample with a metallic mask. Spectra were detected through the micron-size windows: (a) at various excitation powers given near the corresponding curves in μW ($T = 1.6$ K); (b) at various temperatures, shown to the right of the corresponding curves in kelvin. The power of resonant excitation by the Ti–Sp laser is equal to 250 μW.

It is noteworthy that a decrease in the intensity of the I line with increasing temperature is not of the activating origin. Measurements of the temperature dependence of the I-line intensity in different pumping regimes yielded the following relation for its temperature behaviour:

$$I_T \propto (1 - T/T_C), \tag{2}$$

where I_T is the line intensity at given T and T_C is the critical temperature corresponding to the disappearance of this line from the spectrum at given fixed excitation power.

We believe that the above experimental findings are evidence of the Bose condensation of interwell excitons in a lateral trap about 1 μm in size that originates from large-scale fluctuations in random potential. At small excitation powers and sufficiently low temperatures, photoexcited IEs turn out to be strongly localized due to the presence of imperfections (for instance, residual impurities). Corresponding to this situation is a wide, inhomogeneously broadened luminescence band at small excitation powers. But strong dipole–dipole repulsion forbids the localization of more than one exciton on a defect. This accounts for saturation of this luminescence channel in the considered high quality samples at concentrations about or even below 3×10^9 cm^{-2}. A further, above-threshold increase in the pumping intensity in the trap results in the delocalization of interwell excitons (excitation of IEs above the 'mobility edge'). Then, after the critical density values are reached, excitons undergo condensation—macroscopic occupation of the lowest delocalized state in the trap. In our experiments, this transformation is apparent as the appearance, in the threshold manner, of a narrow luminescence line and its superlinear growth close to the threshold region. The most convincing argument in favour of the exciton condensation is the critical temperature dependence on their properties. It is possible to calculate the change in the luminescence intensity of the condensed and supracondensed fractions of the excitons in a micron-scale trapping domain as the temperature increases. Such calculations were performed in [35] and in the framework of the used model the linear behaviour of the intensity of the narrow luminescence line at varying temperature, up to its disappearance from the spectrum, is realized for condensed excitons. At the same

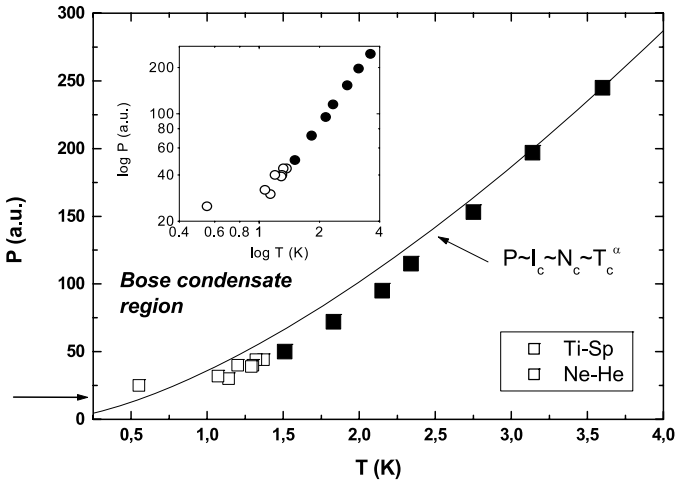

Figure 4. Phase diagram of the Bose condensation of interwell excitons in a lateral trap originated from large-scale random potential fluctuations. Open squares and circles correspond to optical excitation by a Ti–Sp laser, black ones by an Ne–He laser.

time, luminescence of supracondensate excitons displays very low sensitivity to temperature variations in the range under study.

We evaluated the threshold for the appearance of the narrow IE luminescence line corresponding to the onset of macroscopic filling by excitons of the lowest state in the lateral trap. The results were used to construct a phenomenological phase diagram outlining the region of the exciton Bose condensate (figure 4, from [34]). With this aim, we examined pumping dependences of the luminescence spectra in the temperature range 0.5–4 K. For each temperature value in this range, we determined the threshold powers P_C at which the narrow spectral line corresponding to the excitonic condensate either appeared for the first time or began to disappear. In other words, the phase diagram was built in the coordinates P_C–T. The density of interwell excitons was estimated from the 'violet' shift of the line associated with screening of the applied electric voltage at large excitation powers. The threshold exciton density thus found was $n_c = 3 \times 10^{-9}$ cm^{-2} at $T = 0.55$ K (indicated by the arrow in figure 4). The line intensity and exciton concentrations on the pump scale of the phase diagram were linearly related. In the temperature range 1–4 K, the critical density and temperature values at which condensation occurs are related by the power law

$$N_C \approx T^{\alpha}, \tag{3}$$

where $\alpha \geqslant 1$. At $T < 1$ K, the phase boundary cannot be described by a simple power law.

2.2. Interwell exciton luminescence kinetics and spin relaxation

Condensed excitons must be spatially coherent. The spatial coherence should be manifested at least on the scale of the thermal de Broglie wavelength of interwell excitons $\lambda_{ex} \approx h/\sqrt{\pi m_{ex} k_B T}$. At $T = 2$ K, $\lambda_{ex} = 1.5 \times 10^3$ Å, which is one order of magnitude larger than the exciton Bohr radius. The exciton density (n) in the above described experiments corresponded to the dimensionless parameter $r_\lambda = n\lambda_{ex}^2 = 4$. At such special scales, coherent excitons must be phased, i.e. described by the same wavefunction. The development of a collective excitonic state may be accompanied by a rise in the radiative decay rate of condensed excitons compared

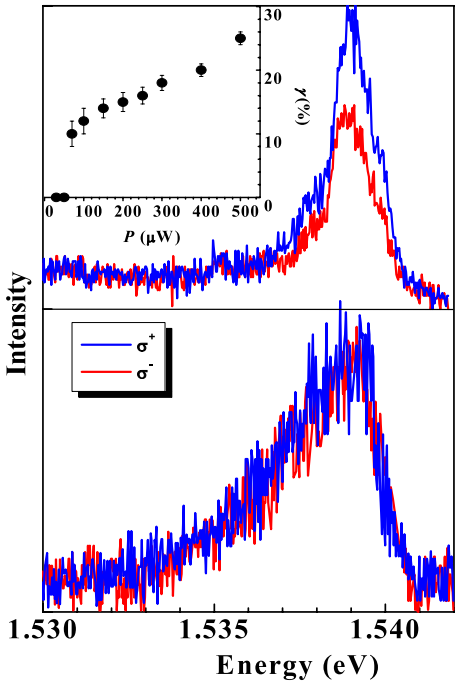

Figure 5. Luminescence of interwell excitons resonantly excited by circularly polarized light. Curves (1) and (2) in the top figure correspond to different circular polarizations, excitation power 150 μW. The luminescence line in the bottom figure (excitation power 60 μW) is not polarized: line contours measured for clockwise and anticlockwise polarization are indiscriminable within the measured noise range. The inset shows the excitation power dependence of the degree of circular polarization γ of the interwell exciton line. $T = 1.7$ K.

with that of supracondensate ones, as well as longer spin relaxation time of condensed excitons than single-particle excitonic spin relaxation [38].

These hypotheses were verified in experiments on the resonant excitation of excitons by polarized light. We recall that the ground state of interwell excitons is not a simple Kramers doublet but is fourfold degenerate with respect to angular momentum projection ($M = \pm 1, \pm 2$). 'Bright' and 'dark' excitonic states are characterized by the respective angular momentum projections $M = \pm 1$ and $M = \pm 2$. In the case of resonant steady-state excitation of an intrawell 1s HH exciton by circularly polarized light, the degree of circular polarization of the IE line corresponding to the condensed phase was found to increase in a threshold manner (figure 5). Enhanced pumping caused a rise in the degree of circular polarization up to 40%. This effect indirectly evidenced a rise in the radiative recombination rate in the condensate and, as well, a possible increase in spin relaxation time. Both were confirmed by direct measurements of the evolution and kinetics of the luminescence spectra under pulsed resonant excitation by circularly polarized light (figures 6 and 7). It follows from figure 6 that the narrow line of the condensed excitonic phase emerged in spectra with a time delay of about 4 ns relative to the excitation pulse. Its decay time was 20 ns, whereas the background continuum under the narrow line 'lived' over 100 ns. Direct measurements of the degree of circular polarization [37] demonstrated that the spin relaxation time of condensed excitons was almost twice as long as the single-particle excitonic spin relaxation measured at $T > T_C$ (figure 7). These results may be regarded as indirect evidence of the enlarged coherent volume of excitonic condensate [38].

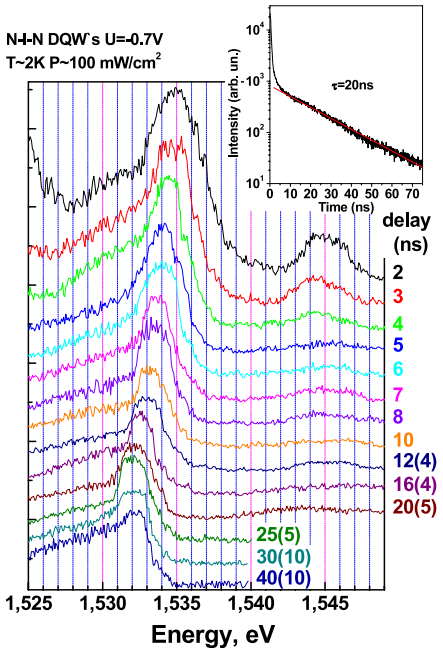

Figure 6. The time evolution of interwell exciton luminescence spectra under pulsed excitation. Numbers to the right of the curves are delay times and signal integration times (in parentheses) in nanoseconds. $T = 2$ K.

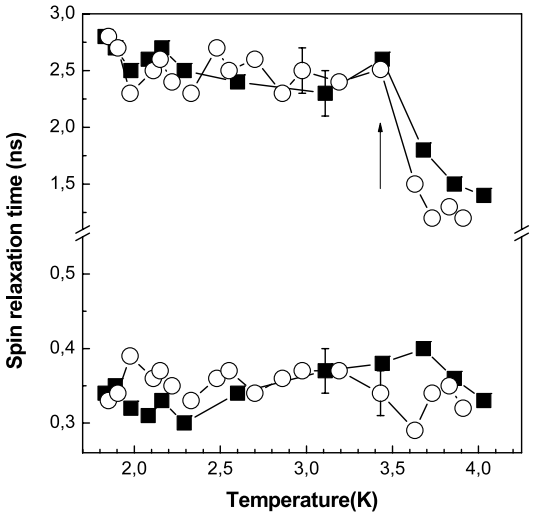

Figure 7. The temperature dependences of spin-relaxation time for intrawell excitons (the lower pair of curves) and interwell excitons (the upper pair of curves). The applied voltage $U = 0.6$ V (circles) and 0.55 V (squares). The arrow indicates the region of abrupt change of spin-relaxation time (from [37]).

Considering the enhanced coherence of the condensed excitonic phase it is worth recalling the interesting experiments of Butov *et al* [19, 21], in which the authors observed an unusual

behaviour of IE photoluminescence kinetics under pulsed laser excitation. At sufficiently high excitation powers and low enough temperature, the kinetics of the IE radiative decay cannot be described by a simple exponential law. Instead, the intensity of photoluminescence increases in a jump-like manner immediately after the pulse excitation and thereafter decreases non-exponentially rapidly. Such unusual behaviour cannot be observed at low excitation power, at high temperatures, in the presence of strong disorder associated with a chaotic potential, or under magnetic field applied perpendicularly to heterolayers. Under such conditions, the photoluminescence kinetics is monoexponential and characterized by a large decay time. We should emphasize that only those delocalized excitons whose translational motion momenta are of the order of the light momentum undergo radiative annihilation, i.e. $\mathbf{K} \leqslant E_g/\hbar c$ (c is the light velocity in the media). The rise in the interwell exciton radiative annihilation observed in [19, 21] is regarded as a result of two effects. One is related to enlargement of the IE coherence area under conditions of exciton condensation to states with smaller momenta than the light ones. The other is assumed to be due to superlinear filling of the optically active excitonic states induced by the stimulated exciton scattering, when the filling numbers in the final exciton states $n \gg 1$ (i.e. as a result of the degenerate Bose statistics of interwell excitons).

2.3. Collective state of Bose gas of interacting interwell excitons in the ring electrostatic traps. Long-range spatial coherence of Bose condensate.

In the case of lateral traps due to chaotic potential, the particular potential trap shape, the actual depth and the lateral size of traps remain uncertain and need to be determined; this leads to the actual problem of artificially creating lateral traps for IEs by means of controlled external impacts, with properties amenable to reliable management and monitoring. Non-uniform electric fields appear to be most suitable for the purpose (see, for example, [39, 40]), in comparison with the method based on non-uniform deformations suggested in [41].

In this section we consider a new series of experiments related to highly spatially resolved luminescence of Bose gas of interacting interwell excitons collected in ring lateral electrostatic traps [42–44]. These experiments have been performed with the use of Schottky-photodiode heterostructures with DQWs and single QWs of the same architecture, as described before. The surface of samples was coated with a metallic Au–Cr mask (thickness around 100 nm) that had circular windows (diameters of the windows were 2, 5, 10, and 20 μm) prepared by electron beam 'lift-off' lithography. Through such windows the photoexcitation and simultaneous microscopic observation of photoluminescence with spatial resolution around 1 μm were performed [42]. In the used Schottky-diode heterostructures the built-in electrode was a 2D electron layer in a wide (30 nm) QW placed at an n-doped buffer layer and a metallic mask was used as a Schottky gate electrode. An electrical bias was applied between the metallic mask and the 2D electron layer. It was found that under applied bias, close to the window edge, a ring lateral trap is formed, where photoexcited dipolar excitons are confined. The behaviour of dipolar excitons confined in the ring lateral traps will be presented and discussed below (see [42–44]).

2.3.1. Schottky-diode heterostructures with double QWs. First we illustrate the quality of the Schottky-diode structures with DQWs employed in our experiments with the example of luminescence spectra of interwell and intrawell excitons obtained when the electric bias across the electrodes was varied. Figure 8 illustrates the evolution of the luminescence spectra under variation of bias voltage. In these experiments, a semitransparent metallic film (Schottky electrode) covered the entire working area of the structure, and the electric field along the structure surface between the electrodes was rather uniform. Luminescence

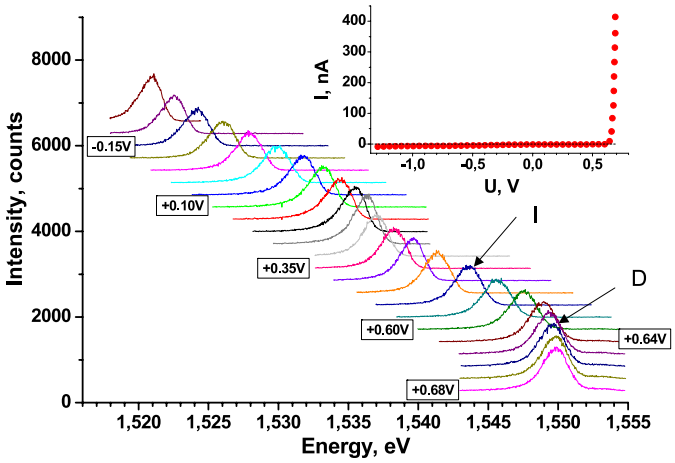

Figure 8. Evolution of the photoluminescence spectra of a Schottky-diode heterostructure with a DQW and a semitransparent electrode deposited atop when lowering the voltage across electrodes from 0.68 to −0.15 V in 0.05 decrements. The He–Ne laser excitation power is $P = 1$ μW. The size of the luminescence excitation spot on the sample is 30 μm. Arrows indicate the luminescence lines of intrawell (D) and interwell (I) excitons. The inset shows the current–voltage characteristic of the structure under investigation. For a voltage above 0.7 V a flat-band condition is realized. $T = 1.7$ K.

photo-excitation and observations were effected through a semitransparent electrode. For a bias voltage $U > 0.7$ V, when a flat-band regime is realized in the structure investigated, the spectrum shows only intrawell exciton luminescence line D. On application of an electric field, the interwell exciton line I emerges with the width 1.7 meV. In accordance with the Stark shift of size quantization levels in QWs, this line moves towards lower energies as a linear function of the applied bias voltage, while the intrawell exciton line drops in intensity to eventually vanish from the spectrum. For spectral shifts exceeding the interwell exciton binding energy by more than an order of magnitude, the intensity of the luminescence line of such excitons remains almost invariable, although their radiative decay time increases considerably with bias. This signifies that non-radiative processes are of little significance in the structures involved and that the structure quality is sufficiently high.

Now let us turn to the experiments in which the window of circular shape on the top of the heterostructures was symmetrically projected just on the entrance split of the spectrometer. This slit cuts only the central part of the symmetrically projected window along its diameter. First of all it was found that under applied bias and photoexcitation the radial distribution of electrical field inside the heterostructure within the window area is strongly non-uniform. Scattered field is minimal in the centre of the window and increases radially to the window edges. But most important, the electric field in the radial direction behaves in a non-monotonic manner close to the circular edge of the window; namely, along the perimeter of the window edge a ring-like potential trap for interwell excitons appears. The existence of such a ring-like potential trap for interwell excitons along the circular edge of the window in the metallic mask was justified by analysis of spectral shifts of the interwell exciton line under scanning of a strongly focused excitation spot in the radial direction in the vicinity of the window edge. The reason for such behaviour of the electric field in the close vicinity of the window in the metallic mask, as well as the behaviour of the shape and the depth of the circular potential trap with applied bias and with conditions of photoexcitation, will be published elsewhere (see also [42, 43]).

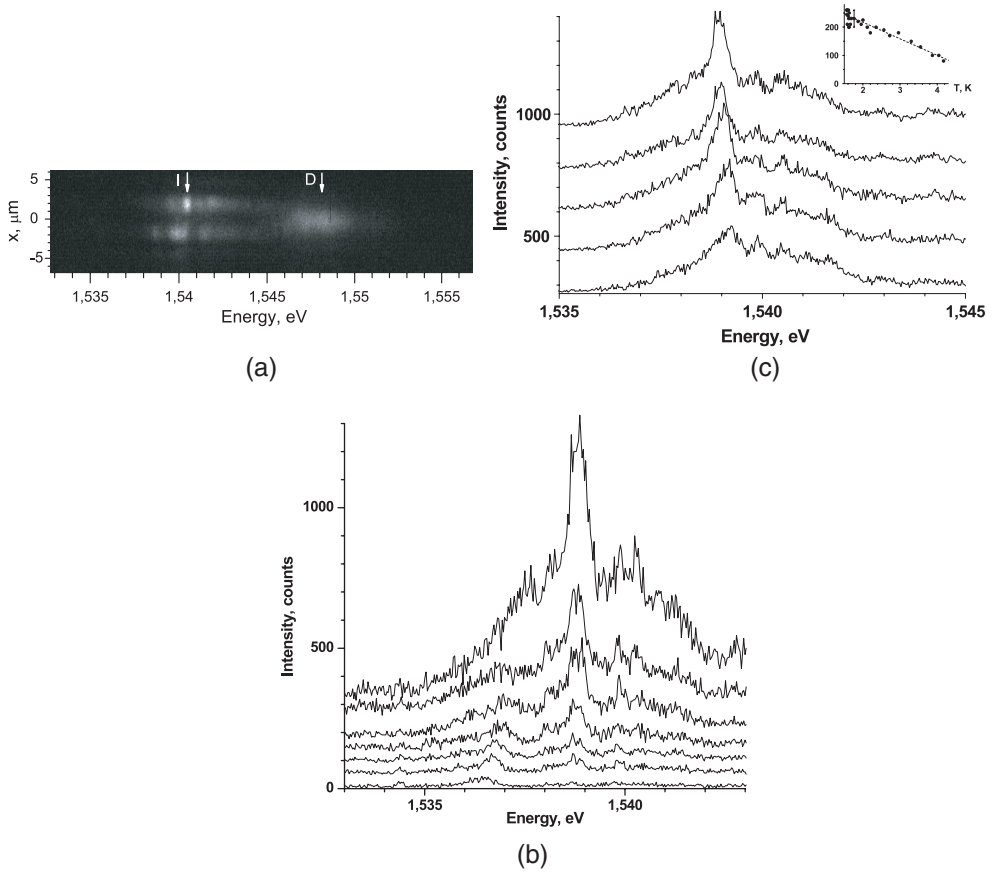

Figure 9. Luminescence spectra measured directly from the 5 μm window in the metallic mask atop of the heterostructure with DQWs; excitation power of Ne–He laser $P_{\mathrm{Ne-He}} = 5$ μW. (a) Space distribution (vertical direction) of photoluminescence within the window; the entrance slit of the spectrometer cut only the central part of the window. (b) Behaviour of the narrow luminescence line corresponding to interwell excitons with excitation power at $T = 1.7$ K; spectra from bottom to top correspond to excitation powers 0.1, 0.2, 0.3, 0.5, 0.75, 1 and 2 μW. (c) Behaviour of narrow interwell luminescence line under temperature variation in the range (1.6–4) K and excitation power 5 μW. Spectra from the top to the bottom measured at temperatures 1.57, 1.58, 2.35, 3.30 and 3.87 K correspondingly. (Inset to (c)) The temperature dependence of the intensity of the narrow interwell exciton line; the dashed straight line represents a linear approximation of this dependence.

A luminescence spectrum from a window of 5 μm size, which is projected just on the entrance slit of the spectrometer, is illustrated in figures 9(a)–(c). The image of interwell exciton luminescence (I) from the window, detected by a CCD camera in the plane of the spectrometer exit slit, is presented in figure 9(a). One can see bright spots of interwell exciton luminescence (spot sizes around 1.5 μm) located at the upper and lower edges of the window. Besides, structureless 'hot' luminescence of the intrawell excitons (D) is seen in the centre of the window where scattered electric field is low. Figure 9(b) demonstrates how a narrow line of an interwell exciton, corresponding to a bright spot, starts to appear and is growing with excitation power increase. This line is placed above the luminescence continuum background connected with localized excitons. Figure 9(c) illustrates the behaviour of this narrow line at given excitation power with temperature increase. One can see the almost linear decrease of the

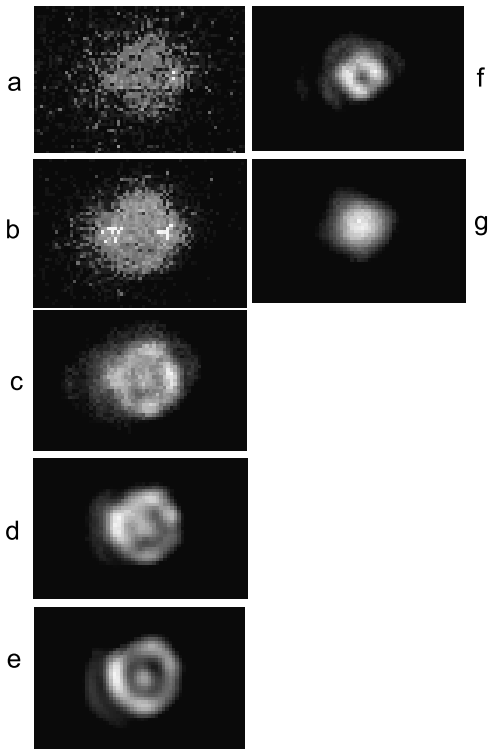

Figure 10. Spatial structure of the interwell exciton luminescence measured from the 5 μm window at $T = 1.7$ K. (a)–(e) (from the top to the bottom in the left column) excitation powers 1, 1.5, 5, 70 and 300 μW with the size of the excitation spot equal to 50 μm. (f) Spatial structure of luminescence in the 2 μm window; (g) luminescence of intrawell excitons.

intensity of the narrow interwell exciton line on temperature increase in the range (1.7–4) K. The data presented in figures 9(b) and (c) are completely equivalent to observations discussed in the previous section 2.1.

Now, let us consider other experiments connected with spatially resolved luminescence when a window of appropriate size was directly projected on the CCD camera avoiding the spectrometer [42]. Under these experiments the luminescence of interwell and intrawell excitons was spectrally and separately selected with the use of interference light filters. Figure 10 presents series of images of the spatially resolved lateral structures of luminescence connected with interwell excitons measured through a 5 μm window at different excitation powers. One can see that at minimal excitation powers, corresponding to average exciton concentration around or less than 10^9 cm^{-2}, the luminescence spot is structureless and its intensity is almost homogeneous within the window under investigation (figure 10(a)). On excitation power increase a discrete luminescence structure starts to appear in a threshold manner along the perimeter of the window. Firstly, two luminescence spots start to appear (figure 10(b)), then four spots (figure 10(c)), then six spots (figure 10(d)); consequently, with excitation power increase spot sizes are around 1.5 μm. At excitation powers around 150 μW the number of spots is equal to eight but very poorly resolved, so the corresponding picture is not exhibited here. Finally, at excitation powers more that 200 μW only structureless luminescence with a ring shape remains visible (figure 10(e)).

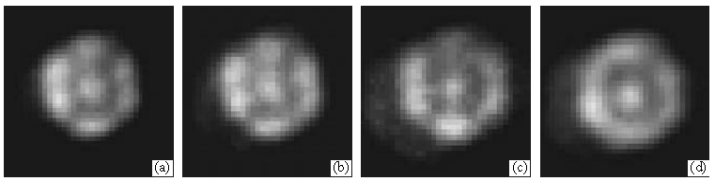

Figure 11. Spatial structure of interwell exciton luminescence in the 5 μm window measured at different temperatures: (a) 1.74 K; (b) 3.9 K; (c) 4.25 K; (d) 4.35 K. Excitation power is 50 μW.

In the case of the 2 μm window the well resolved lateral structure with four equidistantly placed spots is observed (figure 10(f)). In the 10 μm window the lateral structure of the luminescence is more complicated: besides the radially symmetrical structure of the spots the radially symmetrical structures of different rings with spot fragmentation start to be visible. In the case of 20 μm windows we did not observe (perhaps did not resolve) any structures. We should emphasize that luminescence intensity distributions for intrawell excitons under the same experimental conditions remain homogeneous and do not manifest any spatial structure (figure 10(g)).

We should emphasize that the observed geometrical configuration of luminescence spots in figure 10 is aligned along crystallographic direction $\langle 011 \rangle$ in the $\{001\}$ crystallographic plane due to pinning by random potential fluctuations.

For the 5 μm window, taken as an example, the behaviour of a discrete configuration consisting of six equidistant spots was studied under temperature variation at a given excitation power (figure 11). It was established that on temperature increase the discrete luminescence structure starts to wash off (pairs of spots are merging) at $T > 4$ K (see figure 11(d)). Finally, the whole discrete structure of equidistant spots is merged in a continuous luminescent ring at $T \geqslant 15$ K.

It is useful to recall that spatial luminescence distributions of interwell excitons manifested in the form of lateral rings with some fragmented structure along the ring have been observed before by Butov *et al* [45, 46] for the case of DQWs and by Snoke *et al* [47, 48] for a wide single QW. Such ring-like luminescence structures arose under the effect of rather powerful laser excitation. Their origin is related to the depletion of electrons and electric field screening just in the optical pumping region, as well as to the oncoming drift of electrons and holes that occurs under these conditions. Therefore, we believe that there is no direct connection between experiments presented and discussed here and published in [45–48].

The experiments described above were performed on a dozen circular windows with sizes of 2, 5 and 10 μm. But spatial lateral configurations of equidistantly placed luminescence spots in windows of given size and at similar experimental conditions (temperature, excitation power) were always reproduced. This means that the origin of spatially periodical structures of spots manifested in luminescence of interwell excitons laterally confined in a ring trap is an intrinsic property of the interacting dipolar exciton system and is not determined by random potential fluctuations, which definitely exist in investigated samples. In connection with this statement it is worth emphasizing that spatially resolved luminescence of intrawell excitons, measured under the same experimental conditions, was always structureless. As the observed phenomenon is critical to temperature and excitation powers it cannot be mediated by such effects as 'phonon wind' [50, 51], exciton density waves [27] or polariton effects connected with surface plasmons in the vicinity of metallic mask edges.

We believe that the observed phenomenon is the effect of collective coherent properties of interacting dipolar excitons and is a direct consequence of their Bose condensation in a circular lateral trap. To verify this statement we carried out the same sort of experiments but with

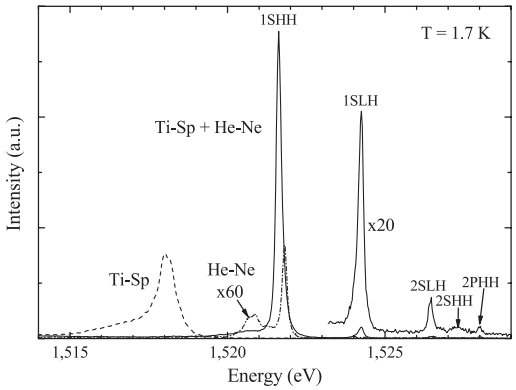

Figure 12. Photoluminescence spectra of Schottky-diode heterostructure with single wide QW (25 nm) and semitransparent atop electrode measured without applied voltage: dotted line, under barrier photo-excitation (Ti–Sp laser, 780 nm, $P = 60$ μW); dashed–dotted line, above barrier photo-excitation (He–Ne laser, 628 nm, $P = 5$ μW); solid line, simultaneous action of these two lasers with the same powers.

the use of another object for investigations of spatially indirect, dipolar excitons, where the influence of uncompensated residual charges on observed phenomena can be eliminated. With this aim a wide (25 nm) single QW subjected to perpendicular electric field in a Schottky-diode heterostructure was used [43, 44].

2.3.2. Schottky-diode heterostructure with single QW. For the first time such structure was investigated in [49] and suggested for studying of dipolar excitons. In a wide QW, where a built-in tunnelling barrier is absent, inhomogeneous broadening of exciton lines is significantly suppressed, which opens opportunity for direct control of residual uncompensated charges in an excitonic system by analysis of relative intensities of free and localized charged excitons (trions). Besides, with the simultaneous use of in-barrier and above barrier photoexcitation and adjusted power proportion between them, it is possible to realize almost complete compensation of residual charge and investigate behaviour of interwell excitons in a 'neutral medium', eliminating effects of Coulomb interaction screening and exciton scattering by charges. Figure 12 illustrates excitonic spectra of a wide QW in a Schottky diode arrangement measured close to a flat band regime through a semitransparent top electrode. With the use of in-barrier cw photoexcitation (780 nm Ti–Sp laser) one can see free direct excitons and recombination connected with a negatively charged channel. With the use of above barrier cw photoexcitation (632.8 nm, Ne–He laser) one can observe a direct free exciton and a broad line connected with a positively charged channel. Under simultaneous use of these two laser sources and adjusted power ratio between them it is possible to photo-excite an almost neutral free excitonic system (figure 12). In this case we observe in spectra only free excitons: a very narrow and intense 1s HH ground state exciton line (dominating in spectra with FWHM close to 0.2 meV) and a small portion of 'hot' luminescence connected with excited excitonic states mediated by heavy and light holes. 'Hot' luminescence of excited excitonic states is visible only when residual charges are maximally compensated. The same procedure of extra charge compensation with the simultaneous use of the above-mentioned photoexcitation sources has been performed under applied bias when dipolar excitons start to appear.

The luminescence spectrum observed in such a structure through a 5 μm window in an atop metallic electrode under applied bias and resonance excitation of 1s HH direct excitons

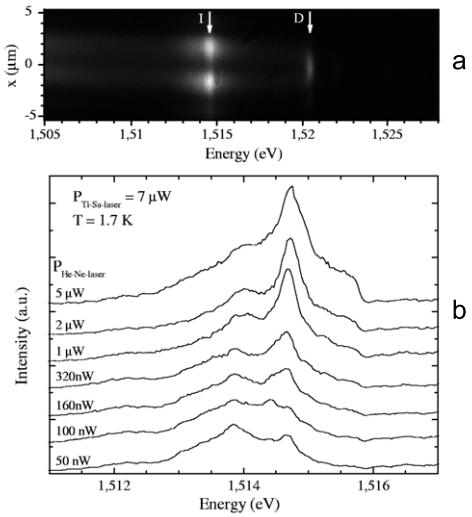

Figure 13. Luminescence spectra of dipolar excitons in Schottky-diode heterostructure with single QW measured with high spatial resolution from 5 μm window in metallic electrode: (a) luminescence spectrum measured with high spatial resolution along entrance spectrometer slit (x-axis), $P_{\mathrm{He-Ne}} = 5$ μW. (b) Behaviour of dipolar exciton line under variation of He–Ne laser power and simultaneous action of resonant photo-excitation by Ti–Sp laser. Applied bias +1.46 V. $T = 1.7$ K.

by a Ti–Sp laser and simultaneous excitation by an Ne–He laser is illustrated in figure 13(a). The enlarged (20×) image of the window was perfectly and symmetrically projected on the entrance slit of the spectrometer with spatial resolution close to 1 μm. Under applied bias one can see two luminescence bright spots shifted to the upper and lower edges of the window and connected with indirect (dipolar) excitons. The intensity distribution in the axial direction, which is almost Gaussian type, reflects the velocity distribution of indirect excitons confined in a trap. It is very interesting to emphasize that just in the centre of each spot a very sharp line (FWHM around 0.2 meV) abruptly appears and grows in intensity with excitation power increase (figure 13(b)). The spatial extension of dipolar exciton luminescence in the radial direction of the trap corresponding to these lines is very narrow (almost 1 μm). The appearance of these sharp lines in a restricted region is attributed to dipolar exciton condensation to the lower state in the trap according to Bose statistics (i.e. macroscopic occupation of the lowest state in the trap).

Now let us consider experiments on spatially resolved luminescence when a window of corresponding size was directly projected on the CCD camera avoiding the spectrometer [43, 44]. Under these experiments the luminescence of dipolar excitons was spectrally selected with the use of an interference filter. Figure 14 presents series of images of the spatially resolved lateral structures of luminescence connected with dipolar excitons measured through a window of 5 μm in size at different excitation powers and $T = 1.6$ K. One can see that at minimal excitation powers, corresponding to average exciton concentration less than 10^9 cm^{-2}, the luminescence intensity within the window is structureless and almost homogeneous (figure 14(a)). On excitation power increase a discrete luminescence structure consisting of four equidistant spots starts to appear in a threshold manner along the perimeter of the window. The intensity redistribution between a pair of spots directed along the diameter was found to increase with excitation power (figures 14(b) and (c)). Spot sizes are around

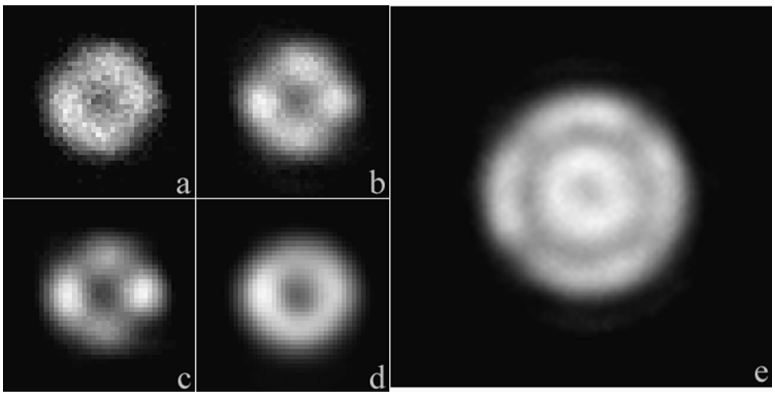

Figure 14. Spatial distributions of dipolar exciton luminescence measured in windows of the Schottky electrode: (a)–(d) window diameter $d = 5\ \mu$m, excitation power of He–Ne laser $P_{\mathrm{He-Ne}} = 0.1$ (a), 2.5 (b), 5 (c) and 250 μW (d); (e) $d = 10\ \mu$m, $P_{\mathrm{He-Ne}} = 10\ \mu$W, $U = +1.46$ V, $T = 1.7$ K. The laser excitation spot on the sample is around 30 μm.

1.5–2 μm. The spot geometrical configuration is aligned along crystallographic direction $\langle 011 \rangle$ in the $\{001\}$ crystallographic plane due to pinning by random potential fluctuations. Finally, at excitation powers above 200 μW only structureless luminescence of a ring shape remains visible (figure 14(d)).

In the 10 μm window the lateral structure of the luminescence is more complicated: besides radially symmetrical equidistant structure of spots radially symmetrical structures of different rings with spot fragmentation start to be visible (figure 14(e)).

For the 5 μm window, taken as an example, the behaviour of a discrete configuration of four equidistant spots was studied under temperature variation at a given excitation power. It was established that on temperature increase the discrete luminescence structure starts to wash off (pairs of spots are merging) at $T > 4$ K. Finally, the whole discrete structure of equidistant spots is merged in a continuous luminescent ring at $T \geqslant 6$ K.

As a diagnostic of Bose condensation of dipolar excitons confined in a lateral trap it is constructive to know the angular distribution of photoluminescence in the direction normal to the 2D plane. If a peak in the photoluminescence in the considered system appeared in the normal to plane direction it would be clear evidence of the long-range coherence of the condensate as shown in [31]. With this aim we performed *in situ* the optical Fourier transformation of the equidistant spot pattern (transformation from real, **r**-, to **k**-space) [43, 44]. Corresponding results are presented in figure 15. The experimentally found Fourier transformations demonstrate the result of destructive and constructive interference. First of all, there is the evidence of long-range spatial coherence of patterned luminescence structure in the real (**r**-space). Second, the luminescence of the condensate is directed normally to the heterostructure plane in a cone with opening angle close to to $\Delta\varphi \cong \lambda/D \cong 0.23$ rad.

Coherent length was measured independently in the straightforward way by means of two-beam interference originated from pairs of luminescence spots elongated to the diameter in the frame (an analogue of classical experiment on amplitude superposition from two independent light sources) [43]. With this aim a magnified image (20×) of patterned luminescence structure in the window was projected just to the plane of crossed slits which could cut any desirable pair of spots in the configuration. An example of two-beam interference from a pair of luminescence spots elongated to the diameter in the frame is presented in figure 16. One can see just in the centre of the interference picture the maximum of zero order (higher interference orders are

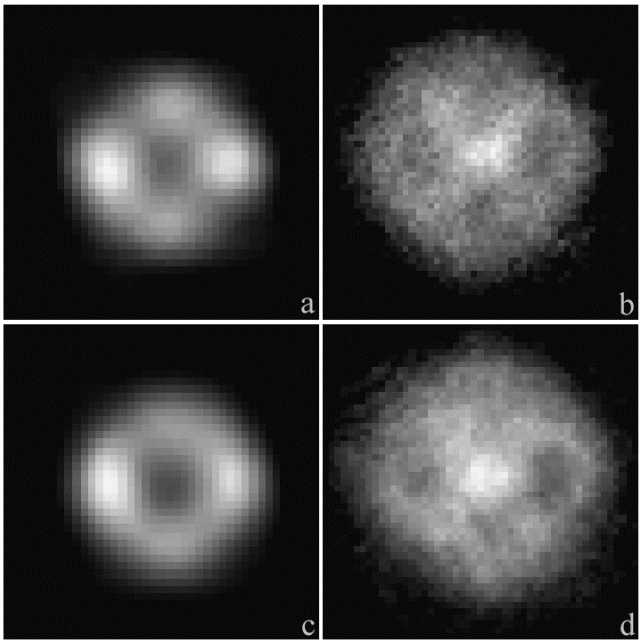

Figure 15. Examples of Fourier transformations (from real—**r**—to **K**-space): (a)–(c) real images of dipolar exciton luminescence from 5 μm window and excitation power 10 and 50 μW; (b)–(d) corresponding Fourier transforms. $T = 1.7$ K, $U = +1.46$ V.

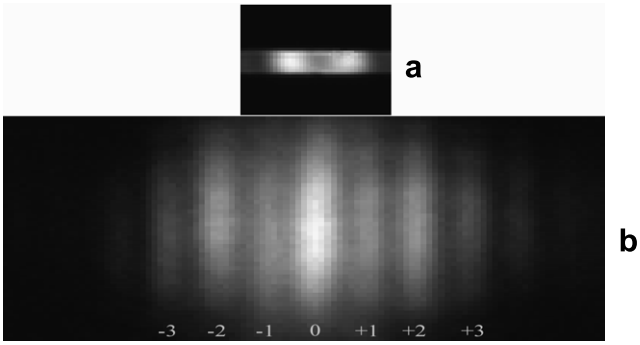

Figure 16. Interference pattern from two luminescence spots elongated to the diameter of the window. (a) Two luminescence spots selected with the use of crossed slits. (b) Interference pattern; corresponding orders are indicated. $T = 1.7$ K; $U = +1.46$ V.

placed symmetrically on right and left sides). Observed interference is due to the first-order coherence of the electric field of the luminescence light emitted by dipolar excitons. From these independent interference experiments it follows that the state of the dipolar exciton Bose condensate is spatially coherent and that the *whole patterned luminescence configuration in real space is described by a common wavefunction*.

Besides, it was found that the intensity of luminescence spots is linearly polarized in the radial direction of the window. Observed polarization can be connected with some tilting of exciton dipole momentum in the radial direction due to asymmetry of the lateral trap in these directions.

Finally, we should emphasize that the observed Bose-condensed state is significantly 'depleted'. By analysis of luminescence intensity we estimate 'depletion' equal to close to 20%.

3. Discussions and conclusion

The phenomenon of Bose condensation discovered in the studied structures emerges in a limited range on the exciton concentration scale: $N_{\rm loc} < N_{\rm ex} < N_{\rm I-M}$. In the low-density region ($N_{\rm loc} \leqslant 10^9$ cm^{-2}), the limitation is imposed by the effects of strong localization on imperfections and in the high-density region ($N_{\rm I-M}$) by disappearance of the bound exciton state caused by the insulator–metal transition. Indeed, a rise in the excitation power above 0.5 mW leads to the broadening of the IE luminescence line in our structures, which continues to be extended and shifts in spectrum to the region of higher energy. The broadening of the I line results from the overlap between the exciton wavefunction in the QW planes and the associated Fermi repulsion between electrons in one QW and holes in another. At an estimated density $N_{\rm I-M} \cong 10^{11}$ cm^{-2}, interwell excitons lose their individual characteristics and the e–h plasma is formed, with electrons and holes specially separated between adjacent QWs. Corresponding to this density is the dimensionless parameter $r_S = 1/(\pi N_{\rm I-M})^{1/2} a_{\rm B} = 1.8$ (the interwell exciton Bohr radius $a_{\rm B} \approx 170$ Å was found from diamagnetic shifts of IEs and by analysis of 'hot' luminescence connected with excited states of interwell excitons). The e–h plasma begins to screen the externally applied electric field, and the interwell luminescence band shifts towards higher energies. It is this shift that was used to find the e–h density.

Presented experiments were performed on a dozen circular windows with sizes 2, 5 and 10 μm in Schottky-diode heterostructures of different architectures (with double and single quantum wells). But spatial lateral configurations of equidistantly placed luminescence spots of dipolar excitons in windows of given sizes and at similar experimental conditions (architecture of heterostructure, temperature and excitation power) were always reproduced. This means that the origin of spatially periodical structures of spots manifested in luminescence of dipolar excitons laterally confined in ring traps is an intrinsic property of an interacting dipolar exciton gas and is not determined by random potential fluctuations. Such chaotic fluctuations definitely exist in investigated samples and pin patterned configurations of spots. In connection with this it worth emphasizing that spatially resolved luminescence of direct excitons, measured under the same experimental conditions, was always structureless. Because observed phenomenon is critical to temperature and excitation powers, it cannot be mediated by such effects as 'phonon wind', exciton density waves or polariton effects connected with surface plasmons in the vicinity of metallic mask edges. We exclude, as well, the interpretation of the observed phenomena in terms of exciton condensation into droplets of dielectric exciton liquid [33], because there are no convincing grounds for coherent binding between such droplets. Besides, we do not see a direct connection of the discovered phenomenon with observations of the luminescence ring formations with some fragmented structure previously published in [45–48].

We assume that the observed phenomenon is the manifestation of collective coherent properties of interacting 2D dipolar excitons and is the direct consequence of their Bose statistics. It is the effect of interwell exciton Bose condensation in a lateral trap of the ring shape. Simple estimates show that dipolar exciton gas when a patterned structure of equidistant spots of micron size appears at realized densities around 2×10^{10} cm^{-2} is degenerated (occupation numbers $n > 1$). A collective exciton state is characterized by a long-range space coherence (coherence length is around perimeter of the ring trap) and is destroyed on temperature increase due to the thermal order parameter fluctuations. In the recently published theoretical studies [31] it was shown that Bose condensation in a trap should be manifested

in a dramatic change of the exciton luminescence angular distribution due to the presence of phase textures in the condensate. In particular, the vortex phase spatial variation of the Bose condensate of the dipolar excitons in a lateral trap leads to a peculiar angle distribution of luminescence intensity due to destructive interference and vortices are imaged by the nodes in the photoluminescence angular profile. In experimentally observed Fourier-transformed images of periodically patterned spots we evidently observe the result of such interference. Besides, this means that the luminescence of the Bose condensate of dipolar excitons is directed normally to the structure plane. It is interesting to mention that expected vortex configurations in real space according to [31] qualitatively coincide with the experimental observations presented above.

We believe that the discovered collective state of a Bose gas of interacting interwell excitons under condensation in circular lateral traps will stimulate further experiments in this interesting area. We assume that due to space coherence of observed periodic structures a temporal beating of luminescence intensity under pulse excitation can be found for weakly coupled condensates (an analogue of Josephson oscillations). Besides, experiments on Bose condensation in lateral traps under pulse resonant photoexcitation with the use of circularly polarized light are expected to be very efficient and informative.

Further improvements of sample quality as well as elimination of uncompensated charges in a system of interacting dipolar excitons are very important and are still in progress. Only with such improvements will further cooling of a dipolar exciton system below 1 K be efficient.

Acknowledgments

We are grateful to A A Dremin and S V Dubonos for significant contribution in the course of these investigations; besides, we are indebted for valuable and stimulating discussions to L V Keldysh, I V Kukushkin, V D Kulakovskii, Yu M Kagan, Yu E Lozovik, S V Iordanskii, L P Pitaevskii and G M Eliashberg.

References

[1] Moskalenko S A 1962 *Sov. Phys.—Solid State* **4** 199
[2] Blatt J M, Boer K W and Brandt W 1962 *Phys. Rev.* **126** 1691
[3] Casella R C 1963 *J. Appl. Phys.* **34** 1703
[4] Keldysh L V and Kopaev Yu V 1965 *Sov. Phys.—Solid State* **6** 2219
[5] Kozlov A N and Maksimov L A 1965 *Sov. Phys.—JETP* **21** 790
[6] Keldysh L V and Kozlov A N 1968 *Sov. Phys.—JETP* **27** 521
[7] Comte C and Nozieres P 1982 *J. Physique* **43** 1069
Comte C and Nozieres P 1982 *J. Physique* **43** 1083
[8] Ketterle W 2002 *Rev. Mod. Phys.* **74** 1131
[9] Hulin D, Mysyrowicz A and Guillaume B C 1980 *Phys. Rev. Lett.* **45** 1970
[10] Snoke D W, Wolfe J P and Mysyrowicz A 1990 *Phys. Rev. Lett.* **64** 2543
[11] Mysyrowicz A, Benson E and Fortin E 1996 *Phys. Rev. Lett.* **77** 896
[12] Lozovik Yu E and Yudson V I 1975 *JETP Lett.* **22** 274
[13] Shevchenko S I 1976 *J. Low Temp. Phys.* **2** 251
[14] Fukuzawa T, Mendez E E and Hong J M 1990 *Phys. Rev. Lett.* **64** 3066
[15] Golub J E *et al* 1990 *Phys. Rev.* B **41** 8564
[16] Kash J A *et al* 1991 *Phys. Rev. Lett.* **66** 2247
[17] Butov L V 1996 *Proc. 23rd Int. Conf. on the Physics of Semiconductors (Berlin, July 1996)* ed M Scheffer and R Zimmermann (Singapore: World Scientific)
[18] Timofeev V B *et al* 1998 *Europhys. Lett.* **41** 535
Timofeev V B *et al* 1998 *JETP Lett.* **67** 613
[19] Butov L V *et al* 1999 *Phys. Rev.* B **59** 1625

[20] Larionov A V *et al* 2000 *JETP Lett.* **90** 1093
[21] Butov L V *et al* 2000 *Phys. Rev.* B **62** 1548
[22] Larionov L V *et al* 2002 *JETP Lett.* **75** 570
[23] Ivanov A L, Ell C and Haug H 1997 *Phys. Rev.* E **55** 6363
[24] Ivanov A L, Littlewood P B and Haug H 1999 *Phys. Rev.* B **59** 5032
[25] Zhu Z, Littlewood P B, Hibersen M S and Rice T M 1995 *Phys. Rev. Lett.* **74** 1633
[26] Yoshioka D and MacDonald A H 1990 *J. Phys. Soc. Japan* **59** 4211
[27] Chen X M and Quinn J J 1991 *Phys. Rev.* B **67** 895
[28] Fernandez-Rossier J and Tejedor C 1997 *Phys. Rev. Lett.* **78** 4809
[29] Lozovik Yu E and Berman O L 1997 *JETP* **84** 1027
[30] Lozovik Yu E and Ovchinnikov I V 2001 *JETP Lett.* **74** 288
[31] Keeling J, Levitov L S and Littlewood P B 2004 *Phys. Rev. Lett.* **92** 176402
[32] Levitov L S, Simons B D and Butov L V 2005 *Phys. Rev. Lett.* **94** 176404
[33] Sugakov V I 2005 *Solid State Commun.* **134** 63
Chernyuk A A and Sugakov V I 2006 *Phys. Rev.* B **74** 085303
[34] Dremin A A *et al* 2002 *JETP Lett.* **76** 450
[35] Gorbunov A V, Bisti V E and Timofeev V B 2004 *JETP* **128** 803
[36] Timofeev V B *et al* 1999 *Phys. Rev.* B **60** 8897
[37] Larionov A V, Bayer M, Hvam J and Soerensen C 2005 *JETP Lett.* **81** 108
[38] Kagan Yu *et al* 2000 *Phys. Rev.* A **61** 043608
[39] Gorbunov A V and Timofeev V B 2004 *JETP Lett.* **80** 185
[40] Rapaport R, Gang C and Simon S H 2006 *Phys. Rev.* B **73** 033319
[41] Snoke D W, Lui Y and Voros Z 2004 *Preprint* cond-mat/0410298 v. 1
[42] Gorbunov A V and Timofeev V B 2006 *Pis. Zh. Eksp. Teor. Phys. (JETP Lett.)* **83** 178
[43] Gorbunov A V and Timofeev V B 2006 *Pis. Zh. Eksp. Teor. Phys. (JETP Lett.)* **84** 390
[44] Timofeev V B and Gorbunov A V 2007 *Invited Talk at ICPS-28 (Wienna, 2006)*; *J. Appl. Phys.* **101** 081708
[45] Butov L V, Lai C W, Ivanov A L, Gossard A C and Chemla D S 2002 *Nature* **417** 47
[46] Butov L V, Gossard A C and Chemla D S 2002 *Nature* **418** 751
[47] Snoke D, Denev S, Lui Y, Pfeiffer L and West K 2002 *Nature* **418** 754
[48] Rapaport R, Chen G, Snoke D, Simon Steven H, Pfieffer L, West K, Liu Y and Denev S 2004 *Phys. Rev. Lett.* **92** 117405
[49] Solov'ev V V *et al* 2006 *Pis. Zh. Eksp. Teor. Fiz. (JETP Lett.)* **83** 647
[50] Keldysh L V 1976 *JETP Lett.* **23** 86
[51] Greenstein M and Wolfe J P 1978 *Phys. Rev. Lett.* **41** 715